Emerging New Climate Extremes Over Europe

Albert Ossó (albert.osso-castillon@uni-graz.at)
Wegener Center for Climate and Global Change, University of Graz https://orcid.org/0000-0001-5653-4886

Richard P. Allan
: University of Reading Department of Meteorology

Ed Hawkins
National Centre for Atmospheric Science

Len Shaffrey
National Center for Atmospheric Science

Douglas Maraun
Wegener Center for Climate and Global Change, University of Graz

Research Article

Keywords: Human society and natural systems, local climate mean and variability, emerging climate signal

Posted Date: March 30th, 2021

DOI: https://doi.org/10.21203/rs.3.rs-359650/v1

Version of Record: A version of this preprint was published at Climate Dynamics on August 16th, 2021.
See the published version at https://doi.org/10.1007/s00382-021-05917-3.

Emerging new climate extremes over Europe

Albert Ossó [1,2], Richard P. Allan[2,3], Ed Hawkins [2,4], Len Shaffrey [2,4] and Douglas Maraun [1]

***Corresponding author*: Albert Ossó, albert.osso-castillon@uni-graz.at**

[(1)] Wegener Center for Climate and Global Change, University of Graz, Graz, Austria

[(2)] Department of Meteorology, University of Reading, Reading, United Kingdom

[(3)] National Centre for Earth Observation, University of Reading, Reading United Kingdom

[(4)] National Centre for Atmospheric Science, University of Reading, Reading, United Kingdom

Abstract

Human society and natural systems are intrinsically adapted to the local climate mean and variability. Therefore, changes relative to the local expected variability are highly relevant for assessing impact and planning for adaptation as the climate changes. We analyse the emerging climate signal relative to the diagnosed internal variability (signal-to-noise ratio, S/N) of a set of recently published climate indices over Europe. We calculate the signal-to-noise ratio with respect to a recent baseline (1951-1983) which relates to recent societal experience. In this framework, we find that during the 2000-2016 period, many areas of Europe already experienced significant changes in climate extremes, even when compared to this recent period which is within living memory. In particular, the S/N of extreme temperatures is larger than 1 and 2 over 34% and 4% of Europe, respectively. We also find that about 15% of Europe is experiencing more intense winter precipitation events, while in summer, 7% of Europe is experiencing stronger drought-inducing conditions.

1. Introduction

Climate change is a global phenomenon, but its impacts differ regionally and seasonally. Societal and natural systems are intrinsically adapted to the local climate in which they are embedded, its mean value and the typical variability range. Exposed to the same mean change, systems adapted to larger variability are usually more resilient than systems that have evolved in more stable climates. For example, for the same temperature increase, tropical ecosystems are generally more vulnerable than extratropical ones, which are adapted to the larger variability of the midlatitudes (*Dillon* et al. 2010; *Mahlstein et al.* 2011; *Frame et al.* 2017; *Harrington et al.* 2016). Therefore, from an impact point of view, it may not be the absolute change but the change relative to the background variability that is especially relevant (*Deutsch et al.* 2008; *Beaumont et al.* 2011). A way to quantify this relation

is by analysing the signal-to-noise ratio (S/N), where the signal (S) is a measure of the mean change of some climate metric respect to a baseline ("the past experience"), and the noise (N) is a representative measure of the variability. The concept of S/N is closely related to the concept of Time of Emergence (ToE) of climate signals (e.g., *Christensen et al.* 2007; *Giorgi and Bi* 2009; *Hawkins and Sutton* 2012; *Maraun* 2013). ToE is the year in which a climate signal emerges from the background variability and is estimated by determining the date on which the S/N ratio permanently crosses a certain threshold. A different perspective is to focus on the S/N value itself on a particular date and try to answer the question: "How familiar or unfamiliar is the current climate in a particular region with respect to the past experience?". In this context, *Frame et al. (*2017) describe how the climate changes with respect to past experience using the terms' unusual' (S/N>1), 'unfamiliar' (S/N > 2) and 'unknown' (S/N > 3). Using these categories, *Hawkins et al.* (2020) calculate the S/N of changes in temperature and precipitation observations and show that many regions are already experiencing a climate that would be unknown by late 19th century standards. Over Europe, changes in temperature and temperature extremes have been detected and attributed partially to anthropogenic influences both in models (e.g., *King et al.* 2015) and observations (*Mahlstein et al.* 2012). *Zhang et al.* (2007) analyses changes in precipitation averaged over latitudinal bands and found that a positive change over northern hemisphere high latitudes is attributable to anthropogenic forcing. *Maraun* (2013) analyses a multi-model ensemble of regional climate projections and found that in northern Europe, positive winter trends in mean and heavy precipitation, and in southwestern and southeastern Europe, summer trends in mean precipitation will emerge within the next few decades. Most of these studies investigate if the trends can be attributed to anthropogenic greenhouse gas forcing, and therefore they use a pre-industrial baseline period. However, due to the lack of high-resolution and homogeneous observational data on pre-industrial times, these studies are based on model data or limit the analysis to a few climate metrics with a relatively coarse spatial resolution. To circumvent this issue, here we analyse how impact-related climate indices have changed in Europe with respect to a more recent baseline (1951-1983). Using a more recent baseline allows us to analyse more climate metrics that are derived from high-quality, high-resolution observational data. The reported changes cannot be directly attributed to anthropogenic forcing. However, we argue that these results are relevant for adaptation planning since they relate with current societal experience, including personal (memory) or practical/technical (most of the European infrastructure has been built after 1950, partially because of the destruction associated with World War II).

2. Methods and data

As in *Hawkins et al.* (2020), we estimate the S/N by regressing local climate variations onto GMST (global mean surface temperature) change

$$L(t) = \alpha G(t) + \beta,$$

where L(t) is the observed local change of some climate metric, G(t) is a smoothed version of GMSTs for the period 1951-2016, and α and β are the parameters of the linear model. We limit the analysis to the period 1951-2016 since this is the period available for the impact-related indices (see description of the indices below).

G(t) is calculated by using monthly-mean near-surface temperature anomalies from the interpolated (gap-filled) HadCRUT4 dataset (*Cowtan et al.* 2014) smoothed with a 15-year running mean (Fig.1). The conclusions are insensitive to whether the smoothing parameter is slightly larger or smaller. The 'signal' of global temperature change (ΔGMST) is defined as the value of the smoothed GMST in 2016 minus smoothed GMST in 1951 (ΔGMST ~ 0.62 K), the component of local climate change explained by GMST (S) is αG, and the 'noise' (N) is defined as the standard deviation of the residuals ($L - \alpha G$). This framework assumes that αG is a good representation of the forced component of the local change. This assumption has been shown to be quite accurate in several studies (e.g., *Sutton et al.* 2015). The statistical significance of the linear regression coefficients is estimated using a two-tailed Student's t-test with adjusted p-values to avoid the overestimation associated with multiple testing (*Wilks* 2016). The p-value adjustment is performed following the false discovery rate test suggested by *Wilks* (2016). We calculate the percentage of area with a S/N over a certain threshold by adding the surface area of the grid points with a statistically significant S/N above the threshold divided by the total area covered by the data.

We estimate the S/N for a set of impact-related indices selected based on their importance for both physical and human environments (see Table 1). The indices analysed are a subset of a new gridded dataset developed in the framework of the ERA4CS INDECIS project (European Union Grant 690462). The indices are available at a 0.25° resolution for the whole of Europe and cover the period 1950-2017. The indices characterise different aspects of the frequency, intensity and duration of extreme events. They are derived from a broad set of climate variables from the European Climate Assessment & Dataset (ECA&D) E-OBS version v17.0e gridded dataset (https://www.ecad.eu/download/ensembles/ensembles.php) and the ERA5 dataset (https://www.ecmwf.int/en/forecasts/datasets/reanalysis-datasets/era5), including surface air temperature and precipitation (from E-OBS) and relative humidity, wind speed, cloudiness and solar radiation from ERA5 (*Castro et al*. 2020). We tested the sensitivity of our results to the use of the E-OBS version v21.0e by calculating the S/N of temperature and total precipitation with this later E-OBS version. For temperature and precipitation, the S/N derived from both versions are virtually identical for the overlapping period and regions (see Figure S1 and S2). Since the indices are derived from temperature and precipitation data from the E-OBS dataset, we do not expect any significant change of our results to a future update of the indices database to the latest E-OBS versions.

3. Results

3.1 S/N of temperature-based indices

3.1.1 Seasonal mean temperatures

Figure 2 shows the surface temperature (Ts) signal, noise and S/N over Europe for different seasonal means. In winter (December, January, February: DJF), the spatial pattern of the signal and noise is characterised by a gradient from the south-west (SW) to north-east (NE) with the largest values over Belarus, western Russia and Scandinavia (Fig. 2a, b). The winter Ts signal is above 1°C over all Europe and up to 3°C in Scandinavia and NE Europe. Interestingly, some regional features depart from the main pattern; in particular, large signals are also observed in the southern Alpine region and southern Italy, where the signals are above 3.5° C. The S/N is larger than 1 over 26% of Europe (Fig. 2c), indicating that a substantial portion of Europe is experiencing unusually warm winter temperatures compared with the 1951-1983 period.

During springtime (March, April, May: MAM), the spatial pattern of the signal and the noise resembles that of winter (Fig.2d,e). The magnitude of the signal is similar to winter, but the noise is about half of the size over central and northern Europe. The smaller noise increases the magnitude of S/N over these areas (Fig.2f). Overall, the S/N of spring temperatures is larger than 1 and 2 over 82% and 3% of Europe, respectively.

In summer (June, July, August: JJA), the largest signals are observed over southern Europe (about 1.5° C), with some areas of southern France, Italy and Spain exhibiting values larger than 2°C (Fig.2g). In contrast, the signal is smaller over Scandinavia and the UK (about 1° C). The spatial pattern of the noise is remarkably homogeneous, and the values are the smallest of the year (Fig. 2d,e). The S/N is larger than 1 over most continental Europe and larger than 2 over large patches of southern Europe and Iberia (Fig.2f). In contrast, the signal has still not "emerged" (S/N<1) in Scandinavia. Overall, the S/N of summer temperatures is larger than 1 and 2 over 50% and 19% of Europe, respectively.

Finally, during autumn (September, October, November: SON), the signal is the smallest of the year and does not have a distinctive spatial pattern (Fig.2j). The noise is larger than in summer, with the largest values over Scandinavia and NE Europe (Fig. 2k). The S/N appears to be dominated by the pattern of the noise, showing S/N values above one over the western half of Europe and generally S/N<1 over NE Europe and Scandinavia (Fig.2l). Overall, the S/N of autumn temperatures is larger than 1 over 45% of Europe.

3.1.2 Extreme temperature indices

Heatwaves are a natural phenomenon often associated with persistent anticyclonic circulation anomalies (e.g., *Trenberth et al.* 2012). However, heatwaves are becoming more intense and occurring more frequently due to anthropogenic global warming (e.g., *Meehl and Tebaldi* 2004; *Perkins et al.* 2012). Heatwaves are among the most dangerous of natural hazards. From 1998 to 2017, it is estimated more than 166,000 people died due to heatwaves associated heat stress (https://www.who.int/health-topics/heatwaves), including more than 70,000 who died during the 2003 heatwave in Europe (*Robine et al.*, 2008). Here, we analyse the S/N of the following extreme temperatures climate indices described in Table 1: warm days (WD), warm nights (WN), very warm days (VWD), warm spell duration (WSD) and the number of days with maximum Ts>32 degrees Celsius (D32). These indices are related to the probability of heatwave occurrence and with the impact of heat on public health. We focus our attention on the summer season (JJA) since it is the season where heat impacts are more relevant.

The S/N of WD is above 1 in most of Europe except over Scandinavia and the UK (Fig. 3a). S/N values above 2 are observed across southern Europe, especially over the Iberian Peninsula, covering about 9% of Europe territory.

Understanding the changes in WN is very important for public health planning since humans need cooler night temperatures to recover. High night temperatures have a substantial contribution to the final death toll of a heatwave (*Trigo et al.* 2005). The S/N of WN (Fig. 3b) is generally larger than for WD, and its distribution is less homogenous. This asymmetry between daytime and nocturnal temperature trends has been observed in several studies and has been attributed primarily to an increase in cloud cover (e.g., *Henderson-Sellers* 1992; *Dessens and Bücher* 1995; *Kaas and Frich* 1995; *Dai et al.* 1999). The highest WN S/N values are found in southern Spain, Italy, the southern Alpine region and eastern Europe. Overall, the S/N of WN is larger than 1 over 51% and larger than 2 and 3 over 20% and 3% of Europe, respectively.

The S/N of VWD is smaller than for WD. It exceeds 1 over central Europe and the Iberian Peninsula, covering about 30% of Europe territory (Fig. 3c).

By construction, the above temperature-related indices describe changes relative to the local climatology. Therefore, the spatial differences in their S/N can be interpreted as a geographically differentiated response to forcing. Overall, the results suggest that the areas more exposed to Atlantic air advection such as NW Europe, Scandinavia and the UK have smaller S/N values. This might be explained by the fact that air temperature change due to global warming is smaller over the oceans than over land (e.g., *Sutton* 2007), so the transport of relatively cool marine air tempers the pace of the warming in comparison to more continental areas.

Fig. 3d show the S/N of D32. D32 is based on a fixed threshold and can be directly related to health concerns. The S/N of D32 is above 1 over large areas of continental Europe except over the mountainous areas of the Alps, the Pyrenees and the Sierra Nevada, where the higher altitudes maintain lower maximum temperatures, and over the NW coast of France, Scandinavia and the UK. Over the Iberian Peninsula, the S/N values are larger, above 2 in central Spain and low-level locations such as the Ebro Depression. Overall, the S/N of D32 is larger than 1 and 2 over 34 % and 4% of Europe, respectively.

The indices analysed above show evidence of a general tendency towards warmer days and nights, which increase the probability of heat-related impacts. However, it is not only the peak temperatures but also the persistence of the heat waves which is relevant. To analyse changes in the persistence of hot events, we show in Fig. 3e the S/N of the WSD index. The S/N of the WSD exhibits a NE tilted meridional dipole with values larger than 1 over southern Europe and below 1 over the rest of Europe. Overall, 19% of Europe exhibits S/N ratios of WSD larger than 1.

3.2 S/N of precipitation-based indices

3.2.1 Seasonal total rainfall

In winter, the spatial pattern of the Total Precipitation (TP) signal is characterised by a west-east tilted meridional dipole, with positive values over northern Europe, especially over western Scandinavia and Scotland and generally negative values in southern Europe, particularly over Spain and Portugal (Fig. 4a). An exception to this large-scale pattern is the Alpine region, which exhibits a significant positive signal as in northern Europe. In spring, the spatial pattern of the signal resembles that of winter, but the magnitudes of both positive and negative signals are smaller and generally not statistically significant (Fig. 4d). In summer, the spatial pattern is also similar to winter and spring, but the magnitudes are about half the values in winter (Fig. 4g). Finally, in autumn, the signal does not show the distinctive west-east dipole pattern, and the magnitudes are small (Fig. 4j). The noise pattern in winter, spring and autumn shows the higher values over the Atlantic facing areas of the continent and over the land area around the Gulf of Genova (Fig. 4b,e,k). This pattern is reminiscent of the first mode of variability of the Atlantic storm track (e.g., *Rogers* 1997; *Pinto et al.* 2009). In summer, the spatial pattern of the noise is more homogeneous (Fig. 4h). The S/N in winter is larger than one and statistically significant only over some parts of Scandinavia, Scotland and the Baltic countries, covering about 13% of Europe. Simultaneously, a tiny area with S/N smaller than -1, denoting the emergence of unusually low precipitation totals, is observed over northwest Italy in winter and spring (Fig. 4c,f). In summer and autumn, virtually all Europe (>99%) exhibits a S/N smaller than one (Fig. 4i,l).

3.2.2 Flood-related indices

Floods have different character depending on the geographical area, antecedent soil moisture, snowmelt, and the triggering meteorological situation (e.g., *Whitfield* 2012; *Arheimer et al.* 2017; *Wasko & Sharma* 2017). For example, on the Mediterranean coast and in Alpine regions, flooding often occurs in the form of flash floods, which are extreme events of short duration (typically a few hours) usually related to intense convective precipitation (*Maddox et al.* 1979; *Marchi et al.* 2010; *Llasat et al.* 2016). In Central Europe, floods are often related to persistent wet periods (e.g., *Muchan et al.* 2015; *Pfleiderer et al.* 2019) that saturate the soil and lead to overflow. In the first case, the precipitation intensity is the most relevant meteorological factor, while in the second is the compound effects of the total amount of precipitation, evapotranspiration and the duration of the wet period, which are more relevant (*Berghuijs et al.* 2019). Here we analyse hydroclimatic indices relevant for both types of events. In particular, we investigate the S/N of the percentage of the total precipitation due to intense raining episodes (R95p) and the maximum 1-day precipitation (Rx1d), both related to the likelihood of flash floods (*Acquaotta et al.* 2019). Finally, we analysed the S/N of the maximum 5-day consecutive precipitation (Rx5d) and the longest wet period (LWP), which are related to the likelihood of large flooding events.

In winter, the R95p signal is positive over most of Europe, although negative values are also observed over northern Italy and west Ukraine (Figure not shown). In 2016, R95p amounts were about 5% larger in central Europe and up to 20% larger in some areas of Scandinavia, Scotland and the eastern Alps compared with the 1951-1983 period. However, the magnitude of the R95p noise is comparable with that of the signal and therefore, the S/N is generally below one except over Scandinavia and Scotland, where the S/N is larger than 1 and above 2 in some locations (Fig. 5a). Overall, 15% of Europe is experiencing unusually intense winter precipitation. In spring, summer and autumn, the signal, noise, and S/N's spatial pattern are similar to that in winter. However, the S/N magnitudes are smaller than one virtually everywhere (not shown). In winter, the S/N of Rx1 is larger than 1 and 2 over Scandinavia, the Baltic countries and Scotland (Fig.5b). Overall, about 14% of Europe is experiencing unusually large amounts of winter daily accumulated precipitation. In spring, summer and autumn, Rx1d S/N values are all well below one (not shown). Finally, the winter S/N of RX5d is very similar to that of R95p. It is smaller than 1 over most of Europe except over some areas of Scandinavia, Scotland, north of Poland and the Baltic countries (Fig. 5c). In winter, 15% of Europe currently experiences unusually large amounts of five-days accumulated precipitation. As for the other two extreme precipitation indices, the S/N values of RX5d are well below 1 for the other seasons (not shown).

Finally, we have also analysed the S/N of LWP (not shown). In all seasons, the S/N is mostly smaller than 1 overall in Europe, suggesting that the persistence of the precipitation events has not changed significantly during the last decades.

3.3 Drought-related indices

The main drivers of hydrological droughts are lack of precipitation, soil moisture deficits and high evapotranspiration, the latter directly linked to high temperatures sustained over an extensive period (*Seneviratne et al.* 2012). Here we analyse the S/N of the standardised precipitation-evapotranspiration index calculated at a 3-month time scale (SPEI3). The SPEI3 index is widely used to characterise the changes in drought associated with climate change (*Serrano et al.* 2009), and it can be interpreted as the number of standard deviations by which the observed anomaly deviates from the long-term mean. We also calculate the S/N of the reference evapotranspiration index (ETO) and the standard precipitation index (SPI3) to help interpret the results. Finally, the S/N of the Longest Dry Period (LDP) is also calculated. The SPEI3 and ETO indices are only available from 1979 to 2017 since the ETO is derived from the ERA5 reanalysis, which covers the period 1979-2020. Therefore, the baseline used for these two indices is 1980-1997 instead of 1951-1983 we used for the rest of the indices. We show results only for summer since this is the only season with significant changes.

In summer, the S/N of SPEI3 depicts a distinct spatial pattern, with negative S/N values (increased drought probability) over the Iberian Peninsula and eastern Europe (S/N<-2) and positive values (reduced drought probability) in some parts of Scandinavia and Scotland (S/N>1) (Fig.6a). However, only a small fraction of values in the south of the Iberian Peninsula and eastern Europe are statistically significantly different from zero. Figure 6c suggests that the summer drying in southern and southeastern Europe is dominated by a substantial increase in ETO, which shows S/N values larger than 1 over most Continental Europe and larger than 2 and 3 over Spain and southeastern Europe. In contrast, the SPEI3 S/N increase over Scotland and Scandinavia appears to be driven by the positive changes in SPI3 (increased precipitation) over these areas. Overall, 27%, 16%, and 5% of Europe show S/N values of ETO above 1, 2 and 3. However, changes in drought probability relative to the 1951-1983 period have not yet emerged (not shown). Finally, the LDP S/N values are well under one everywhere in all seasons (figure not shown).

4. Conclusions

The S/N ratio of observed surface temperatures, precipitation and a set of impact-related climate indices associated with flooding, drought and extreme temperature have been investigated for

the period 1951-2016 to evaluate how changes in climate metrics of direct relevance to society are emerging above the envelope of recent societal experience (1951-1983).

We have shown evidence that large parts of Europe are experiencing more severe climate extremes. Figure 7 illustrates schematically the most relevant summer and winter changes. Table 2 shows the percentage of European territory where the S/N of different climate indices cross a certain threshold. The results indicate that summer episodes of extreme daily maximum temperatures have become more frequent over more than 55% of Europe. The changes in extreme (warm) night temperatures are even more extensive, with more than 74% of the European territory showing an emerging signal. S/N values above 1 in D32 (days with maximum temperature above 32°C) are also observed over large parts of Continental Europe, and S/N values above 2 are shown in the Iberian Peninsula. These results indicate that millions of people are currently experiencing unfamiliarly high temperatures, even compared to the recent past.

The flood-related climate indices analysis shows that the noise of precipitation and extreme precipitation time series is high, and over about 90% of Europe, the signal has not yet emerged in any season. However, some northern Europe areas, Scandinavia and Scotland, show the emergence of stronger winter precipitation events during winter.

Similarly to the flood-related indices, we found that the drought signal has only emerged over some reduced areas of southeastern Europe and the Iberia Peninsula driven by large increases in the levels of potential evapotranspiration, which is much higher than in our baseline period (1951-1983) over most continental Europe.

Our analysis shows an earlier emergence and larger S/N rations of temperature and precipitation extremes than found in other studies that used an earlier baseline period (e.g., *King et al.* 2015; *Maraun* (2013); *Mahlstein et al.* (2012); *Zhang et al.* (2007)). It is important to note that 1950-1970 was a relatively cool period due to anthropogenic aerosol, and therefore the magnitude of the signals is potentially amplified when using our baseline period.

The analysis of the observed S/N ratio of climate indicators with respect to a recent baseline provides useful and easily distillable information to many socio-economic sectors. The methodology used in this manuscript can be applied to more sector-specific indicators such as heat stress indicators, agricultural indicators (e.g., length of the growing season), snow days and snowmelt for ski tourism, to enumerate a few. To achieve such aims, it is necessary to continue monitoring the European climate and these indices operationally.

Declarations

Funding

This work was funded by the INDECIS project which is part of ERA4CS, an ERA-NET initiated by JPI Climate, and funded by FORMAS (SE), DLR (DE), BMWFW (AT), IFD (DK), MINECO (ES), ANR (FR) with co-funding by the European Union Grant 690462).

Conflicts of interest/Competing interests

The authors have no conflicts or competing interests.

Availability of data and material

The data is freely available at the following repositories: Indices: http://indecis.eu/ EOBS: https://www.ecad.eu/download/ensembles/ensembles.php.

Code availability

The code is available upon request.

Acknowledgements

This work was funded by the INDECIS project which is part of ERA4CS, an ERA-NET initiated by JPI Climate, and funded by FORMAS (SE), DLR (DE), BMWFW (AT), IFD (DK), MINECO (ES), ANR (FR) with co-funding by the European Union Grant 690462).

References

Acquaotta, F., Faccini, F., Fratianni, S. et al. Increased flash flooding in Genoa Metropolitan Area: a combination of climate changes and soil consumption? Meteorol Atmos Phys 131, 1099–1110 (2019). https://doi.org/10.1007/s00703-018-0623-4

Arheimer, B., Donnelly, C. & Lindström, G. Regulation of snow-fed rivers affects flow regimes more than climate change. Nat Commun 8, 62 (2017). https://doi.org/10.1038/s41467-017-00092-8

Beaumont, L. J., A. Pitman, S. Perkins, N. E. Zimmermann, N. G. Yoccoz, and W. Thuiller, Impacts of climate change on the worlds most exceptional ecoregions, Proceedings of the National Academy of Sciences, 108 (6), 2306– 2311, doi:10.1073/pnas.1007217108, 2011.

Berghuijs, W. R., Harrigan, S., Molnar, P., Slater, L. J., & Kirchner, J. W. (2019). The relative importance of different flood-generating mechanisms across Europe. Water Resources Research, 55, 4582– 4593. https://doi.org/10.1029/2019WR024841

Christensen, J. H., et al. (2007), Regional climate projections, in Climate Change 2007: The Physical Science Basis, edited by S. Solomon et al., pp. 847–940, Cambridge Univ. Press, Cambridge, U. K.

Cornes, R., G. van der Schrier, E.J.M. van den Besselaar, and P.D. Jones. 2018: An Ensemble Version of the E-OBS Temperature and Precipitation Datasets, J. Geophys. Res. Atmos., 123. doi:10.1029/2017JD028200"

Cowtan, K. and Way, R.G. (2014), Coverage bias in the HadCRUT4 temperature series and its impact on recent temperature trends. Q.J.R. Meteorol. Soc., 140: 1935-1944. doi:10.1002/qj.2297

Dai, A., K. E. Trenberth, and T. R. Karl, 1999: Effects of Clouds, Soil Moisture, Precipitation, and Water Vapor on Diurnal Temperature Range. J. Climate, 12, 2451–2473. https://doi.org/10.1175/1520-0442(1999)012<2451:EOCSMP>2.0.CO;2.

Dessens, J., and A. Bücher, 1995: Changes in minimum and maximum temperatures at the Pic du Midi in relation with humidity and cloudiness. Atmos. Res., 37, 147–162. https://doi.org/10.1016/0169-8095(94)00075-O.

Deutsch, C. A., J. J. Tewksbury, R. B. Huey, K. S. Sheldon, C. K. Ghalambor, D. C. Haak, and P. R. Martin, Impacts of climate warming on terrestrial ectotherms across latitude, Proceedings of the National Academy of Sciences, 105(18), 6668–6672, doi:10.1073/pnas.0709472105, 2008.

Dillon, M., Wang, G. & Huey, R. Global metabolic impacts of recent climate warming. *Nature* **467,** 704–706 (2010). https://doi.org/10.1038/nature09407.

Domínguez-Castro, F., Reig, F., Vicente-Serrano, S.M. et al. A multidecadal assessment of climate indices over Europe. Sci Data 7, 125 (2020). https://doi.org/10.1038/s41597-020-0464-0.

Fischer, E. M., and Knutti, R. (2014), Detection of spatially aggregated changes in temperature and precipitation extremes, *Geophys. Res. Lett.*, 41, 547– 554, doi:10.1002/2013GL058499.

Frame, D., Joshi, M., Hawkins, E. et al. Population-based emergence of unfamiliar climates. Nature Clim Change 7, 407–411 (2017). https://doi.org/10.1038/nclimate3297.

Giorgi, F., and Bi, X. (2009), Time of emergence (TOE) of GHG-forced precipitation change hot-spots, *Geophys. Res. Lett.*, 36, L06709, doi:10.1029/2009GL037593.

Harrington, R., Fleming, R.A. and Woiwod, I.P. (2001), Climate change impacts on insect management and conservation in temperate regions: can they be predicted?. Agricultural and Forest Entomology, 3: 233-240. doi:10.1046/j.1461-9555.2001.00120.x."

Harrington, L. J., Frame, D. J., Fischer, E. M., Hawkins, E., Joshi, M., & Jones, C. D. (2016). Poorest countries experience earlier anthropogenic emergence of daily temperature extremes. *Environmental Research Letters*, *11*(5), 055007.

Hawkins, E., and Sutton, R. (2012), Time of emergence of climate signals, Geophys. Res. Lett., 39, L01702, doi:10.1029/2011GL050087.

Hawkins, E., Frame, D., Harrington, L., Joshi, M., King, A., Rojas, M., & Sutton, R. (2020). Observed emergence of the climate change signal: From the familiar to the unknown. Geophysical Research Letters, 47, e2019GL086259. https://doi.org/10.1029/2019GL086259

Henderson-Sellers, A. Continental cloudiness changes this century. *GeoJournal* **27,** 255–262 (1992). https://doi.org/10.1007/BF02482666

Kaas, E., and P. Frich, 1995: Diurnal temperature range and cloud cover in the Nordic countries: Observed trends and estimates for the future. Atmos. Res., 37, 211–228. https://doi.org/10.1016/0169-8095(94)00078-R

King, A. D., et al., 2015: The timing of anthropogenic emergence in simulated climate extremes. Environ. Res. Lett., 10, 094015, https://doi.org/10.1088/1748-9326/10/9/094015.

Llasat, M. C., Marcos, R., Turco, M., Gilabert, J., & Llasat-Botija, M. (2016). Trends in flash flood events versus convective precipitation in the Mediterranean region: The case of Catalonia. Journal of Hydrology, 541, 24-37. https://doi.org/10.1016/j.jhydrol.2016.05.040.

413 Maddox, R.A., C.F. Chappell, and L.R. Hoxit, 1979: Synoptic and Meso-α Scale Aspects of Flash
414 Flood Events. Bull. Amer. Meteor. Soc., 60, 115–123, https://doi.org/10.1175/1520-0477-60.2.115
415
416 Mahlstein, I., Knutti, R., Solomon, S., & Portmann, R. W. (2011). Early onset of significant local
417 warming in low latitude countries. *Environmental Research Letters*, *6*(3), 034009.
418
419 Mahlstein, I., G. Hegerl, and S. Solomon, 2012: Emerging local warming signals in observational
420 data. Geophys. Res. Lett., 39, n/a-n/a, https://doi.org/10.1029/2012GL053952.
421
422 Maraun, D., 2013: When will trends in European mean and heavy daily precipitation emerge?
423 Environ. Res. Lett., 8, 14004, https://doi.org/10.1088/1748-9326/8/1/014004.
424
425 Marchi, Lorenzo, et al. "Characterisation of selected extreme flash floods in Europe and implications
426 for flood risk management." Journal of Hydrology 394.1-2 (2010): 118-133.
427 https://doi.org/10.1016/j.jhydrol.2010.07.017.
428
429 G.A. Meehl, C. Tebaldi More intense, more frequent, and longer lasting heat waves in the 21st
430 century, Science, 305 (5686) (2004), pp. 994-997. DOI: 10.1126/science.1098704.
431
432 Muchan, K., Lewis, M., Hannaford, J. and Parry, S. (2015), The winter storms of 2013/2014 in the
433 UK: hydrological responses and impacts. Weather, 70: 55-61. doi:10.1002/wea.2469
434
435 S.E. Perkins, L.V. Alexander, J.R. Nairn Increasing frequency, intensity and duration of observed
436 global heatwaves and warm spells Geophys. Res. Lett., 39 (20) (2012), 10.1029/2012GL053361
437
438 Pfleiderer, P., Schleussner, C. F., Kornhuber, K., & Coumou, D. (2019). Summer weather becomes
439 more persistent in a 2 °C world. Nature Climate Change, 9(9), 666–671.
440 https://doi.org/10.1038/s41558-019-0555-0
441
442 Pinto, J.G., Zacharias, S., Fink, A.H. *et al.* Factors contributing to the development of extreme North
443 Atlantic cyclones and their relationship with the NAO. *Clim Dyn* **32,** 711–737 (2009).
444 https://doi.org/10.1007/s00382-008-0396-4
445
446 Robine, J. M. et al. Death toll exceeded 70,000 in Europe during the summer of 2003. C. R. Biol.331,
447 171–178 (2008). https://doi.org/10.1016/j.crvi.2007.12.001.

Rogers, J. C., 1997: North Atlantic Storm Track Variability and Its Association to the North Atlantic Oscillation and Climate Variability of Northern Europe. *J. Climate*, **10**, 1635–1647, https://doi.org/10.1175/1520-0442(1997)010<1635:NASTVA>2.0.CO;2.

Seneviratne, S. Historical drought trends revisited. Nature 491, 338–339 (2012). https://doi.org/10.1038/491338a

Sutton, R., E. Suckling, and E. Hawkins, What does global mean temperature tell us about local climate? Philosophical Transactions of the Royal Society A: Mathematical, Physical and Engineering Sciences, 373(2054), 20140,426, doi:10.1098/rsta.2014.0426, 2015.

Sutton, R. T., Dong, B., and Gregory, J. M. (2007), Land/sea warming ratio in response to climate change: IPCC AR4 model results and comparison with observations, *Geophys. Res. Lett.*, 34, L02701, doi:10.1029/2006GL028164.

Trenberth, K. E., and Fasullo, J. T. (2012), Climate extremes and climate change: The Russian heat wave and other climate extremes of 2010, J. Geophys. Res., 117, D17103, doi:10.1029/2012JD018020.

Trigo, R. M., García-Herrera, R., Díaz, J., Trigo, I. F., and Valente, M. A. (2005), How exceptional was the early August 2003 heatwave in France? Geophys. Res. Lett., 32, L10701, doi:10.1029/2005GL022410.

Vicente-Serrano, S. M., Beguería, S., & López-Moreno, J. I. (2010). A Multiscalar Drought Index Sensitive to Global Warming: The Standardized Precipitation Evapotranspiration Index, *Journal of Climate*, *23*(7), 1696-1718. Retrieved Mar 14, 2021, from https://journals.ametsoc.org/view/journals/clim/23/7/2009jcli2909.1.xml

Wasko, C., Sharma, A. Global assessment of flood and storm extremes with increased temperatures. *Sci Rep* **7,** 7945 (2017). https://doi.org/10.1038/s41598-017-08481-1

Whitfield, P. (2012), Changing floods in future climates. J. Flood Risk Manage, 5: 336-365. doi:10.1111/j.1753-318X.2012.01150.x

483 Zhang, X., Zwiers, F., Hegerl, G. *et al.* Detection of human influence on twentieth-century
484 precipitation trends. *Nature* **448,** 461–465 (2007). https://doi.org/10.1038/nature06025
485

Table 1. Definitions of the indices used in this study. The abbreviations and definitions follow Castro et al. 2020.

Index Code	Index Name	Description	Units	Reference
Rx1d	Maximum one-day precipitation	Highest precipitation amount in one-day period	mm/month	Klein Tank AMG et al. 2009
Rx5d	Maximum consecutive 5-day precipitation	Highest precipitation amount in five-day period	mm/month	Klein Tank AMG et al. 2009
R95tot	R95t	Precipitation due to very wet days (> 95th percentile) divided by total precipitation	%	Klein Tank AMG et al. 2009
LWP	Longest wet period	Maximum length of consecutive wet days (RR*>=1)	days/ month	Klein Tank AMG, ZwiersFW, Zhang X. 2009
LDP	Longest dry period	Maximum length of consecutive dry days (RR<1)	days/month	Gregory J. McCabe, et al, 2010
SPEI3	SPEI3	Standardised precipitation-evapotranspiration index calculated at 3-month time scale	Standardised units	Vicente-Serrano et al. 2010
SPI3	SPI3	Standardised precipitation index calculated at 3-month time scale	Standardised units	McKee, T. B et al. 1993
ETO	Reference Evapotranspiration	If data available using Fao-56 Penman-Monteith, if not using the Hargreaves & Samani method.	mm/month	Chiew, F.H.S et al. 1995
WD	Warm days	Total numbers of days with TX** higher than the 90th percentile	days/month	Klein Tank AMG, Zwiers FW, Zhang X. 2009
WN	Warms nights	Total numbers of days with TN*** higher than the 90th	days/month	Klein Tank AMG, Zwiers FW, Zhang

		percentile		X. 2009
D32	Temperature sums above 32 ℃(duration)	Number of days with TX≥32 ℃	days/month	Klein Tank AMG, Zwiers FW, Zhang X. 2009
WSD	Warm spell duration	Count of days with at least 6 consecutive days when TX > 90thpercentile	Days/season	Klein Tank AMG, Zwiers FW, Zhang X. 2009

*RR Daily precipitation, ** TN: Minimum daily temperature, *** TX: Maximum daily temperature.

Table 2*:* Percentage of the total European area with S/N values of the indicated indices over a specific threshold (only statistically significant values are used to calculate the area).

INDICES DJF	**1 ≥ SN < 2**	**2 ≥ SN < 3**	**3 ≥ SN < 4**
Ts	26 %	~ 0 %	~ 0 %
RT	13 %	0 %	~ 0 %
Rx1d	7 %	7 %	~ 0 %
Rx5d	15 %	0 %	~ 0 %
R95	15 %	0 %	~ 0 %
INDICES JJA	**1 ≥ SN < 2**	**2 ≥ SN < 3**	**3 ≥ SN < 4**
Ts	50 %	19 %	1 %
WD	44 %	9 %	~ 0 %
WN	51 %	20 %	3 %
VWD	30 %	~ 0 %	~ 0 %
D32	34 %	4 %	~ 0 %
WSD	19 %	~ 0 %	~ 0 %
SPEI3	3 %	4 %	~ 0 %
SPI3	~ 0 %	~ 0 %	~ 0 %
ETO	27 %	16 %	5 %

Figures

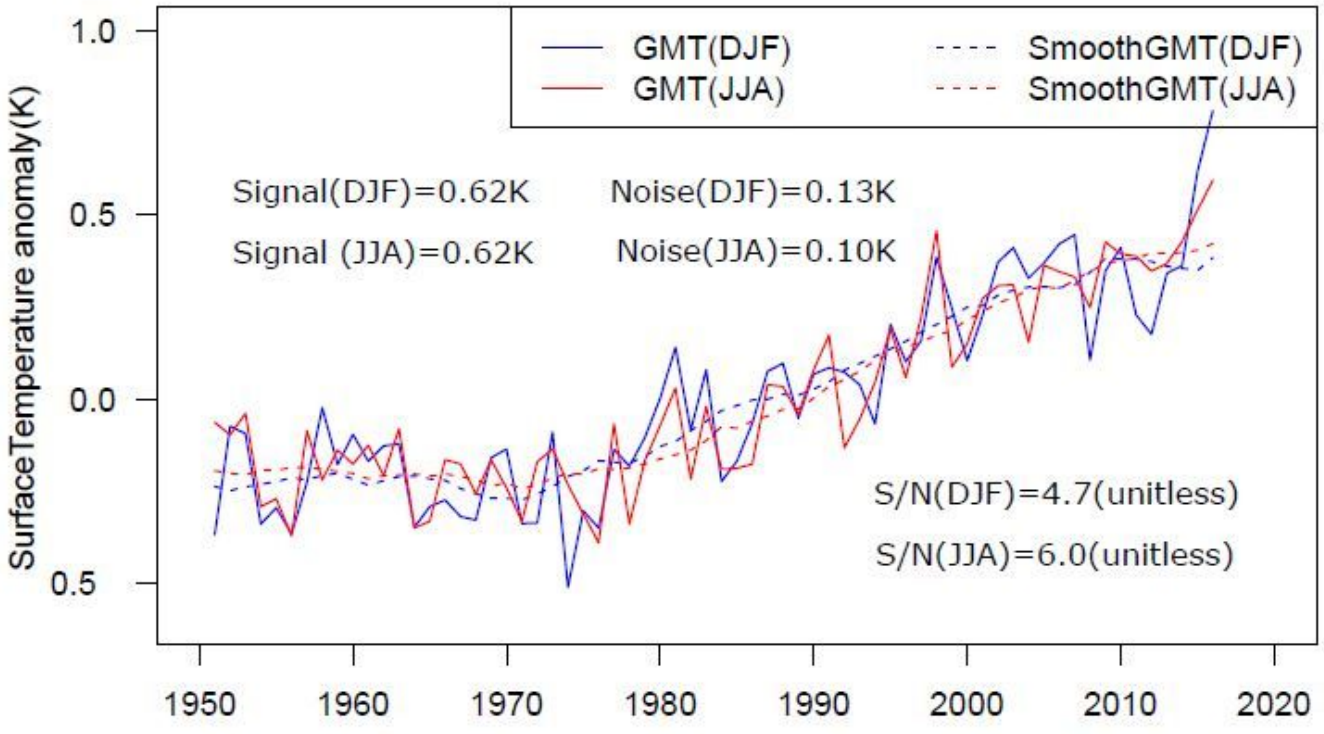

Figure 1

Winter (blue) and summer (red) global mean temperature (GMT) anomaly for the period 1951-2016. The dash lines are running means of the GMT with a time window of 15 years.

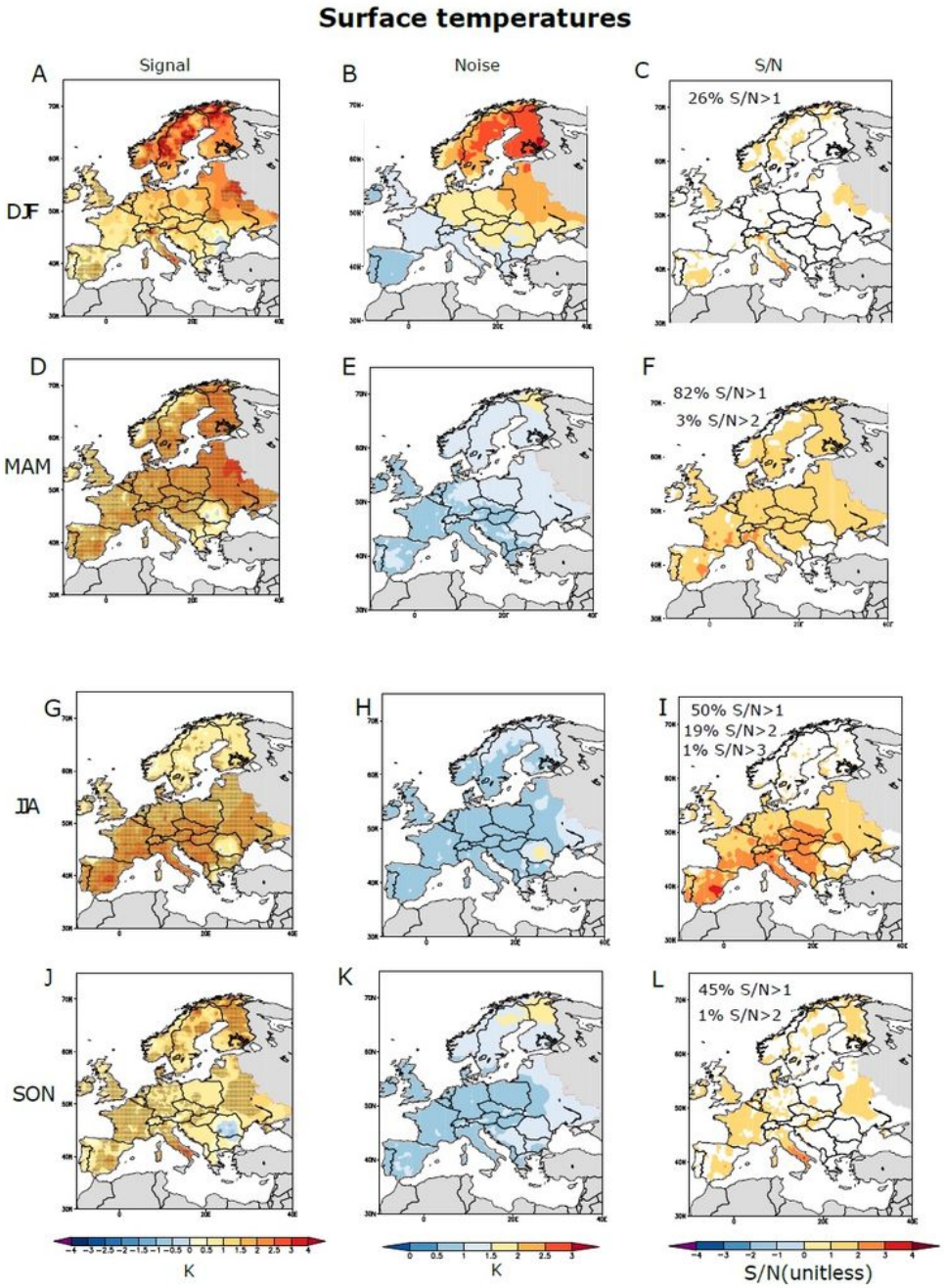

Figure 2

Signal (K), noise (K) and signal-to-noise (unitless) of seasonally averaged surface temperature anomalies (1951-2016) in the EOBS V17 dataset. Grey regions indicate a lack of sufficient data. Stippling in the signal plots (left column) indicates signal values statistically significantly different from zero. Only S/N values statistically significantly from zero are shown (right column). Note: The designations employed and the presentation of the material on this map do not imply the expression of any opinion whatsoever

on the part of Research Square concerning the legal status of any country, territory, city or area or of its authorities, or concerning the delimitation of its frontiers or boundaries. This map has been provided by the authors.

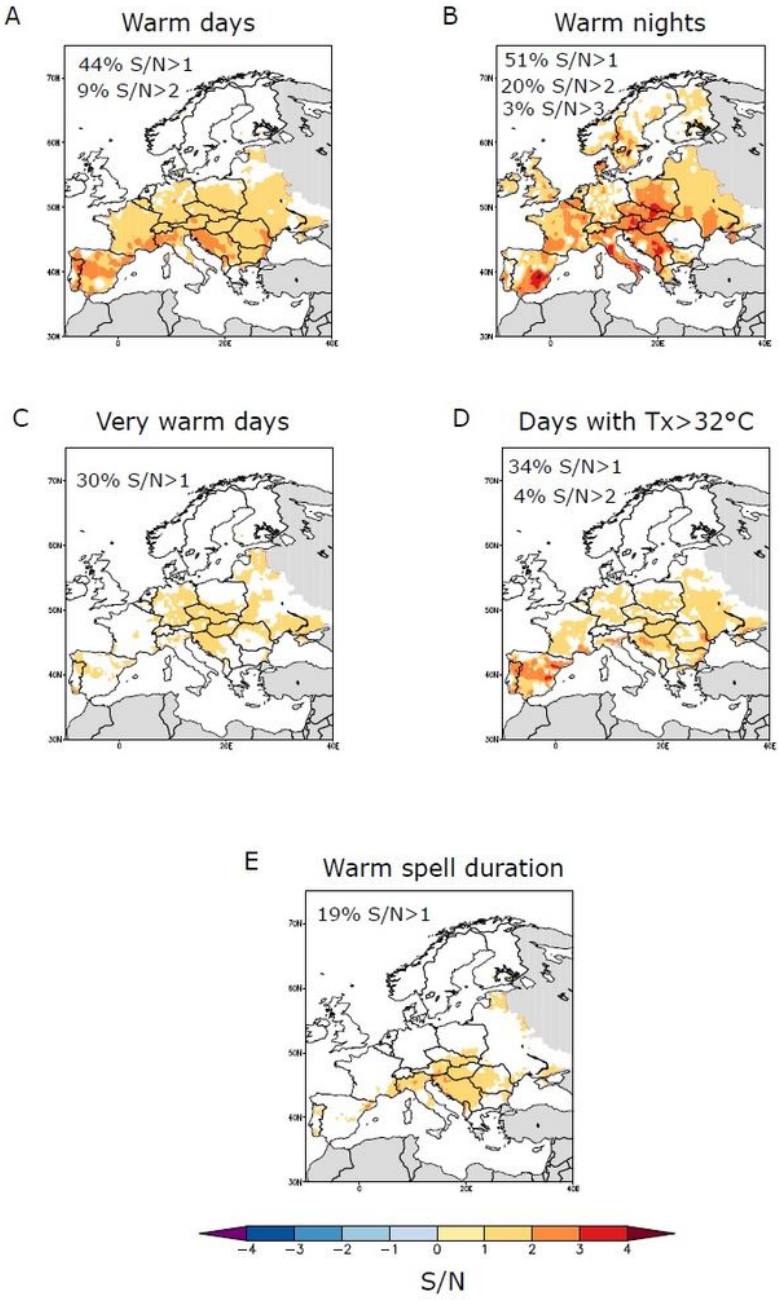

Figure 3

Signal-to-noise ratio (S/N) of summer (JJA) mean extreme temperature climate indices. Grey regions indicate a lack of sufficient data. Only values statistically significantly different from zero are shown.

Note: The designations employed and the presentation of the material on this map do not imply the expression of any opinion whatsoever on the part of Research Square concerning the legal status of any country, territory, city or area or of its authorities, or concerning the delimitation of its frontiers or boundaries. This map has been provided by the authors.

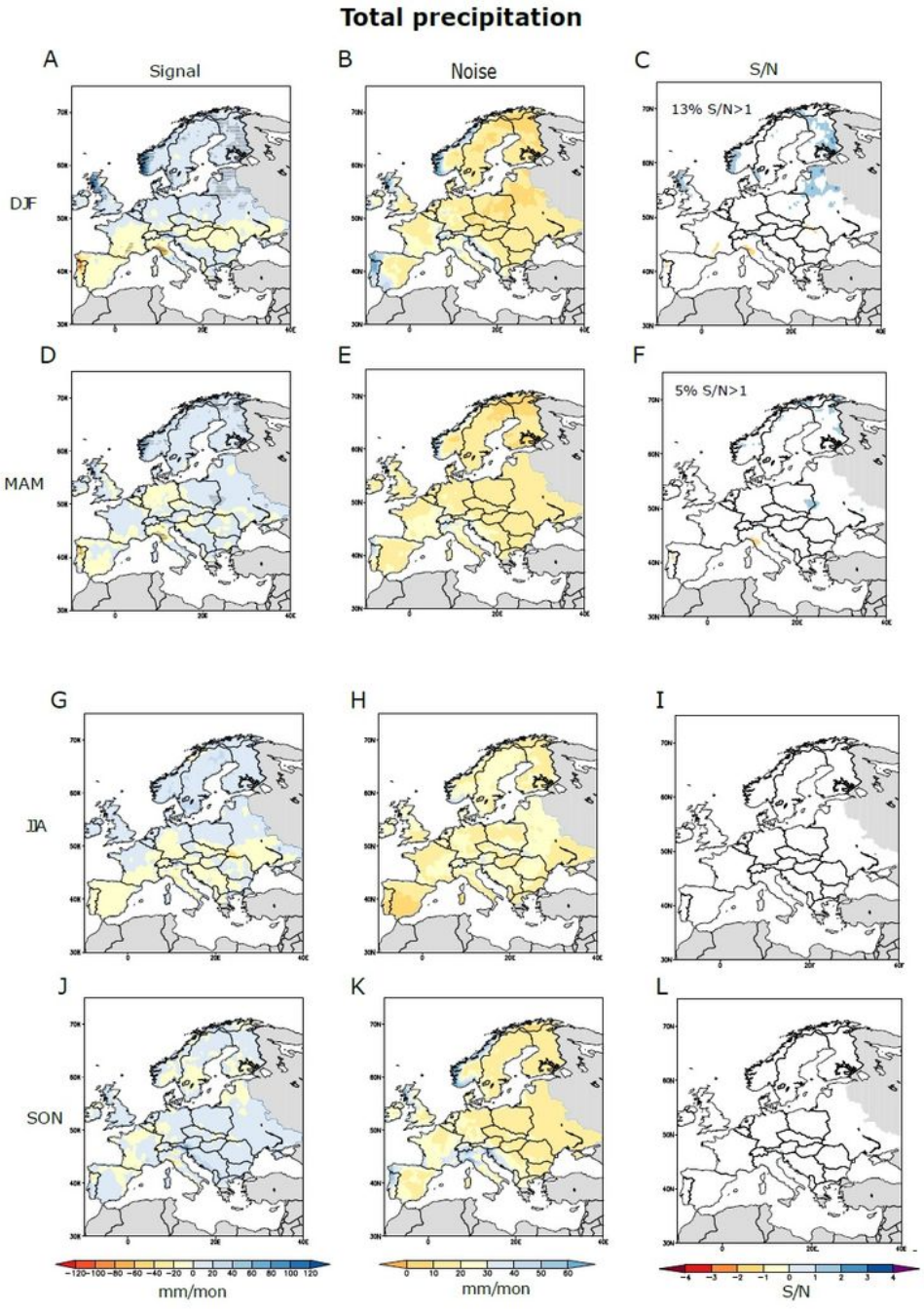

Figure 4

As in figure 2 but for total precipitation anomalies. Note: The designations employed and the presentation of the material on this map do not imply the expression of any opinion whatsoever on the part of Research Square concerning the legal status of any country, territory, city or area or of its authorities, or concerning the delimitation of its frontiers or boundaries. This map has been provided by the authors.

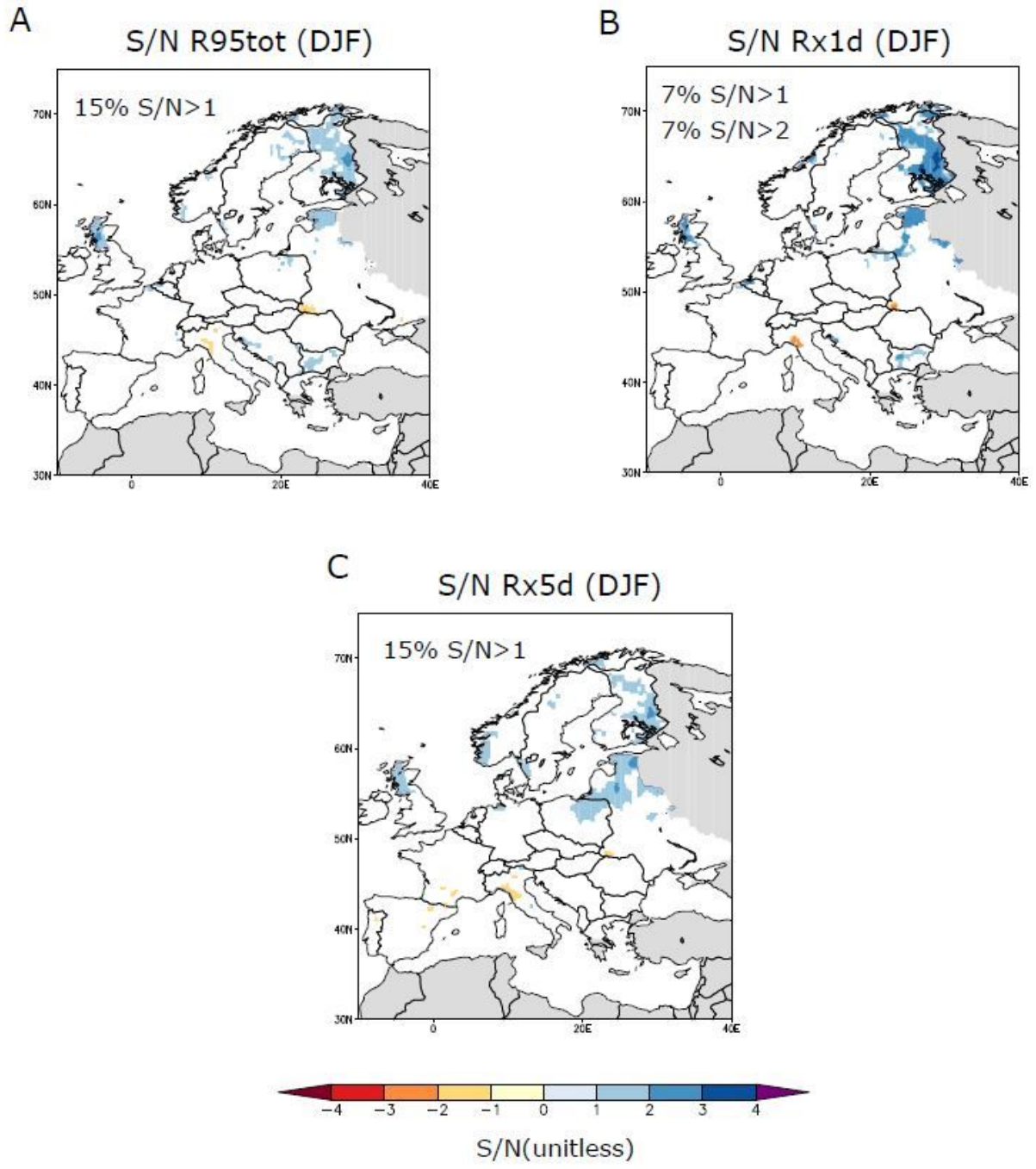

Figure 5

Signal-to-noise ratio (S/N) of winter extreme precipitation indices. Grey regions indicate a lack of sufficient data. Only values statistically significantly different from zero are shown. Note: The designations employed and the presentation of the material on this map do not imply the expression of any opinion whatsoever on the part of Research Square concerning the legal status of any country,

territory, city or area or of its authorities, or concerning the delimitation of its frontiers or boundaries. This map has been provided by the authors.

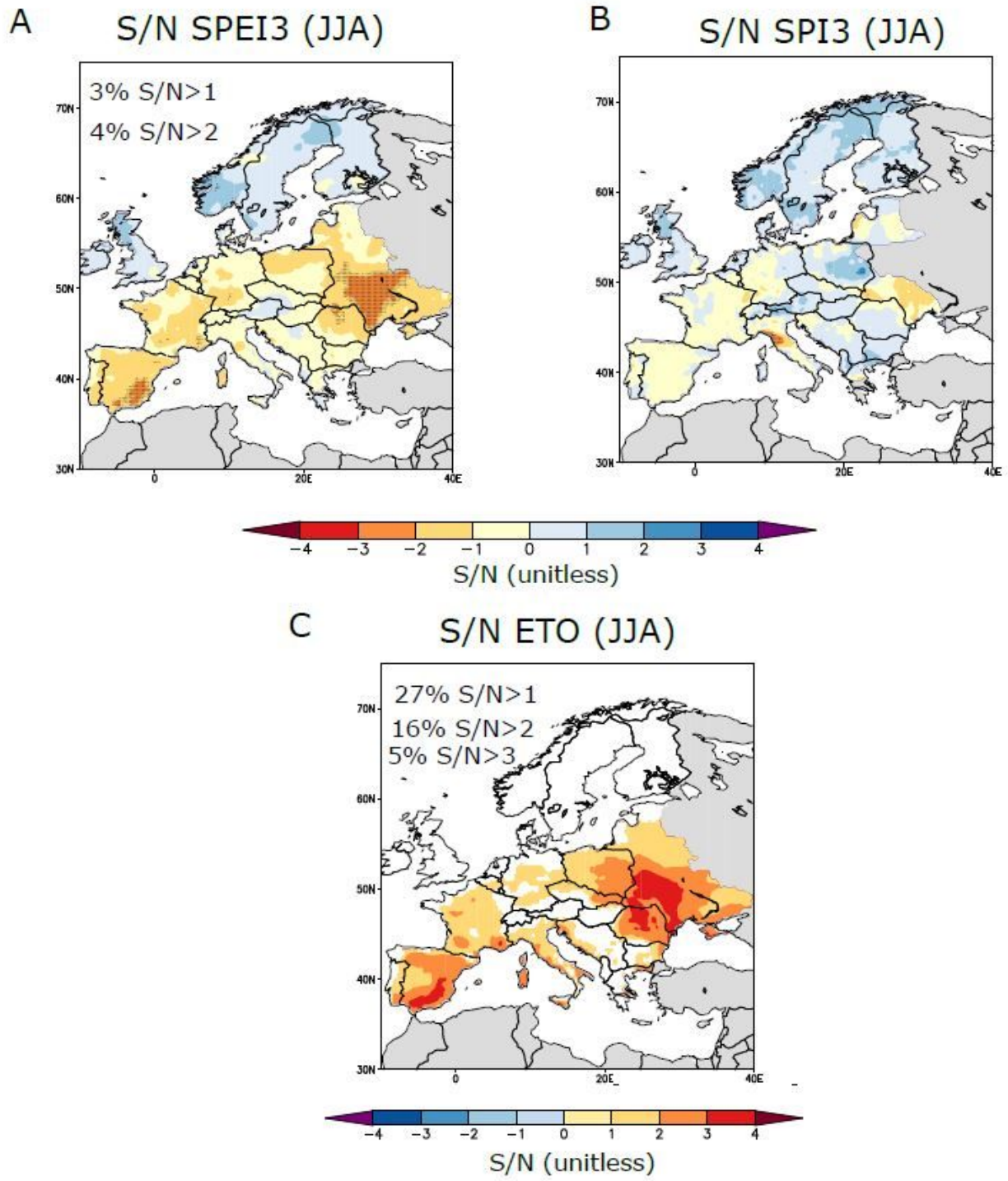

Figure 6

Signal-to-noise ratio (S/N) of summer drought-related indices. Grey regions indicate a lack of sufficient data. Stippling in figures (A) and (B) indicate values statistically significantly different from zero. In figure (C), only values statistically significantly different from zero are shown. Note: The designations employed and the presentation of the material on this map do not imply the expression of any opinion whatsoever on the part of Research Square concerning the legal status of any country, territory, city or area or of its

authorities, or concerning the delimitation of its frontiers or boundaries. This map has been provided by the authors.

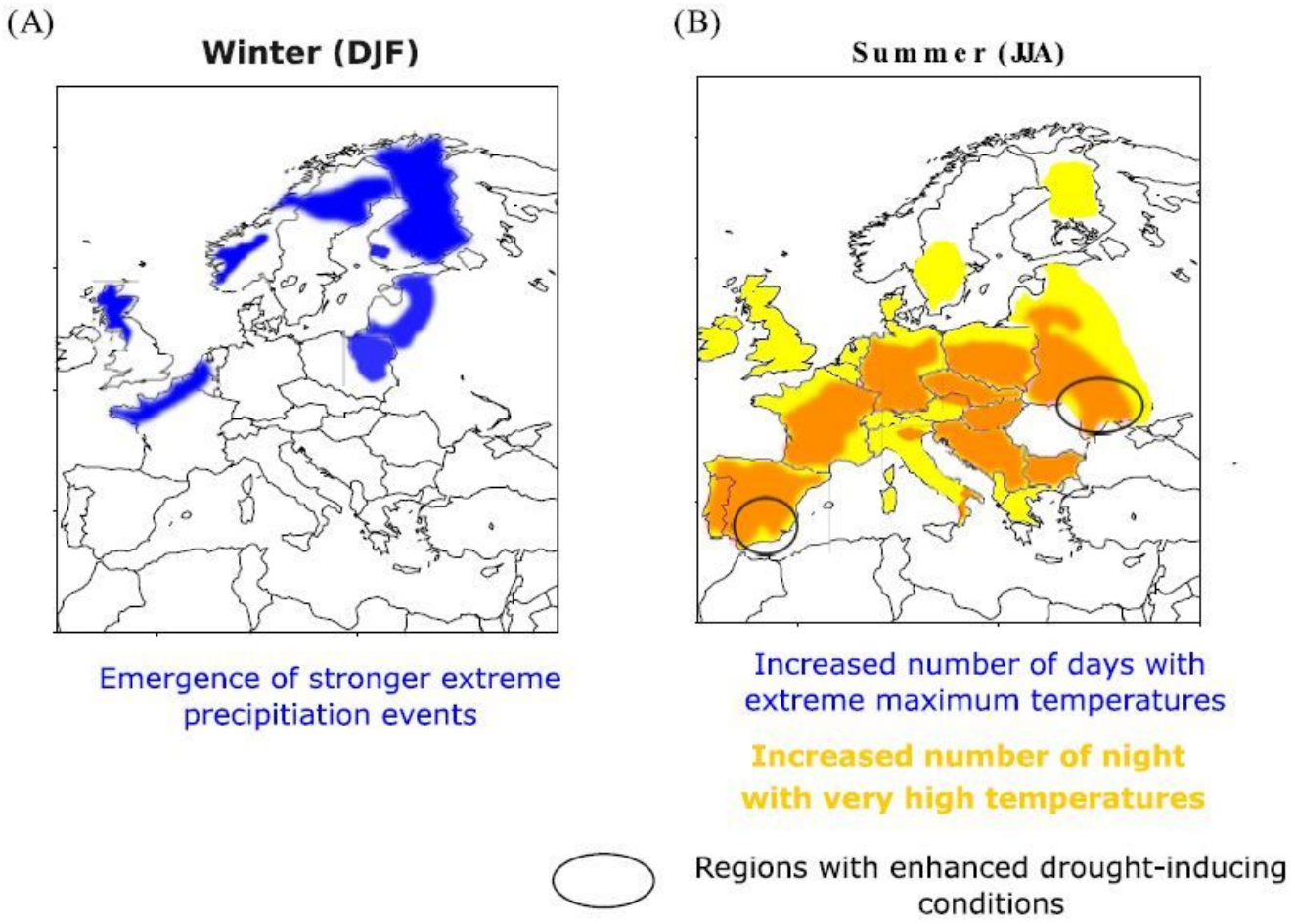

Figure 7

please see the manuscript file for the full caption Note: The designations employed and the presentation of the material on this map do not imply the expression of any opinion whatsoever on the part of Research Square concerning the legal status of any country, territory, city or area or of its authorities, or concerning the delimitation of its frontiers or boundaries. This map has been provided by the authors.

Supplementary Files

This is a list of supplementary files associated with this preprint. Click to download.

- FigureS1.pdf
- FigureS2.pdf